Light meson spectra and chiral quark cluster models

L. A. Blanco, F. Fernández, and A. Valcarce
Grupo de Física Nuclear, Universidad de Salamanca, E-37008 Salamanca, Spain
(Received 16 June 1998)

We study the low-energy spectra of light mesons in the framework of constituent quark models. Several interactions including chiral symmetry breaking and designed for the description of the nucleon-nucleon system and/or the baryon spectra are used. We find that chiral quark models only based on Goldstone boson exchanges are not able to provide a reasonable description of the light meson spectra. However, if they are supplemented with a color-spin term, like the one present in the one-gluon-exchange or instanton-induced potentials, they reproduce in a satisfactory manner the light meson spectra at the same time that they are able to explain the main features of the baryon spectra and the baryon-baryon interaction. [S0556-2813(99)05301-7]

PACS number(s): 12.39.Jh, 14.40.−n, 24.85.+p

Nonrelativistic quark models, relying on simple quark-quark potentials inspired by QCD, provided a surprisingly satisfactory description of baryons and mesons as bound states of constituent quarks [1] as well as the main properties of the baryon-baryon interaction [2]. In fact, they work even much better than one would naively expect by judging on the basis of the nonrelativistic approximation inherent to them. Above all, they allow us to gain some insight into the nature of the forces between quarks beyond what can be learned from just computing numerically a bound-state or a scattering problem.

The basic idea of these models is to consider hadrons as clusters of confined nonrelativistic quarks carrying a constituent mass and interacting through residual interactions coming from QCD. This interaction was originally based on perturbative QCD, realized through the one-gluon exchange (OGE) potential [3], and later on it was obtained from nonperturbative aspects through instanton-induced potentials [4]. The force which confines the quarks is still not well understood, although it is assumed to come from the long-range nonperturbative properties of QCD [5].

Despite their success, all these models lack several important properties. From a phenomenological point of view, neither the OGE potential nor the instanton-induced forces provide the required medium- and long-range interaction to explain the two-baryon experimental data. From a more fundamental point of view, in their original formulation these models violate an underlying symmetry of the QCD Lagrangian: chiral symmetry. Nowadays it is recognized that the constituent quark mass and chiral symmetry are concepts closely related [6,7]. The constituent quark mass appears as a direct consequence of spontaneous chiral symmetry breaking, being related to the generation of quark condensates on the QCD vacuum. An important effect of the spontaneous breakdown of chiral symmetry is the existence of Goldstone bosons which could provide the required missing parts of the interaction between quarks.

This theoretical progress has renewed interest for constituent quark models. Several groups have proposed different schemes to derive models of constituent quarks including chiral symmetry breaking and applied them to the nucleon-nucleon interaction [8–10] or to the baryon spectra [11–13]. Among these chiral quark models one finds mainly two different approaches. In the first one, QCD short-range perturbative effects are maintained through the OGE potential and combined with the nonperturbative effects provided by the breaking of chiral symmetry [8,9,11,12]. The second approach prefers to neglect the OGE and therefore its spin-color dependence, the full interacting Hamiltonian being given only by Goldstone boson exchanges [10,13]. This second approach has been successfully applied to study problems that were previously understood based only on the OGE potential plus confinement, like, for example, the baryon spectra. It has also been used to explain the short-range repulsion of the NN interaction [10], usually attributed to the quark substructure of hadrons and explained some time ago through OGE dynamics [14]. Therefore, it raises the question of whether the spin-color operator is actually needed in a Hamiltonian constructed at the level of quarks or if the Goldstone boson exchanges alone are able to provide a correct description of the hadron spectra and the baryon-baryon interaction.

Assuming that both the baryon spectra and the baryon-baryon interaction can be equally well described within the two approaches (let us note that the only trials in this direction have been based on chiral quark models including simultaneously OGE and Goldstone boson exchanges [11,12]) one has to resort to another system in order to disentangle whether only Goldstone boson exchanges can account for the phenomenology. If the nonrelativistic realization of the low-energy QCD is valid, this system might be the meson spectra.

Thus, our purpose in this work is to test these chiral quark models, mainly used for the nucleon-nucleon interaction and the baryon spectra, in order to describe the meson spectra. This problem has been widely studied in the past by means of QCD-inspired models using either OGE potentials [15] or instanton-induced interactions [16–18], but as stated before none of these models is able to describe the baryon-baryon phenomenology.

We will use three of the standard chiral quark cluster models present in the literature [8,9,13]. One can find the rationale for these models in the instanton liquid picture of the QCD vacuum [19,20]. Light quarks interacting with the

instanton vacuum develop a nonzero momentum-dependent dynamical (constituent) mass. It means that chiral symmetry breaks down spontaneously and does not manifest itself in multiplets of particles, but through the appearance of Goldstone fields. Calculating n-point correlation functions of pseudoscalar densities in the instanton vacuum, Diakonov and Petrov [20] were able to construct an effective low-energy Lagrangian

$$L_{\rm eff}=\overline{\Psi}_f^{\alpha}[i\gamma^{\beta}\delta_{\beta}-M(q^2)e^{i\gamma_5\vec{\tau}\vec{\phi}/f_{\pi}}]_{fg}\Psi_g^{\alpha}, \tag{1}$$

where $\Psi_{f(g)}^{\alpha}$ is the spinor of the quark, α is the color index, f and g are flavor indices, and $M(q^2)$ is the quark dynamical mass. This mass can be parametrized as [8,11]

$$M(q^2)=f_{\pi}g_{\rm ch}\left[\frac{\Lambda_{\rm CSB}^2}{\Lambda_{\rm CSB}^2+q^2}\right]^{1/2}, \tag{2}$$

where $\Lambda_{\rm CSB}$ acts as an ultraviolet cutoff of the (nonrenormalizable) effective theory [20].

Working in the spirit of the SU(2)⊗SU(2) linear sigma model, Fernández *et al.* [8] have derived from the Lagrangian of Eq. (1) a quark-quark interaction containing a pseudoscalar ($V_{\rm PS}$) and a scalar ($V_{\rm S}$) potential provided by the exchange of Goldstone bosons. Besides, the potential model includes an effective one-gluon exchange interaction which simulates the short-range perturbative QCD behavior and a confinement potential which provides the nonperturbative QCD effects in the long distance and confines three quarks to a baryon or a $q\overline{q}$ pair to a meson. The qq interaction includes the following terms:

$$V_{qq}(\vec{r})=V_{\rm OGE}(\vec{r})+V_{\rm CON}(\vec{r})+V_{\rm PS}(\vec{r})+V_{\rm S}(\vec{r}), \tag{3}$$

where

$$V_{\rm OGE}(\vec{r})=\frac{1}{4}\alpha_s(\vec{\lambda}_i\vec{\lambda}_j)\left[\frac{1}{r}-\frac{\pi}{m_im_j}\left(1+\frac{2}{3}(\vec{\sigma}_i\cdot\vec{\sigma}_j)\right)\delta(\vec{r})\right], \tag{4}$$

$$V_{\rm CON}(\vec{r})=-a_c(\vec{\lambda}_i\vec{\lambda}_j)r^2, \tag{5}$$

$$V_{\rm PS}(\vec{r})=\alpha_{ch}\frac{\Lambda_{\rm CSB}^2}{\Lambda_{\rm CSB}^2-m_{\pi}^2}\frac{m_{\pi}}{3}\times\left[Y(m_{\pi}r)-\frac{\Lambda_{\rm CSB}^3}{m_{\pi}^3}Y(\Lambda_{\rm CSB}r)\right]\times(\vec{\sigma}_i\cdot\vec{\sigma}_j)(\vec{\tau}_i\cdot\vec{\tau}_j), \tag{6}$$

$$V_{\rm S}(\vec{r})=-\alpha_{ch}\frac{4m_q^2}{m_{\pi}^2}\frac{\Lambda_{\rm CSB}^2}{\Lambda_{\rm CSB}^2-m_{\sigma}^2}m_{\sigma}\times\left[Y(m_{\sigma}r)-\frac{\Lambda_{\rm CSB}}{m_{\sigma}}Y(\Lambda_{\rm CSB}r)\right]. \tag{7}$$

Reference [9] employs a generalized chiral symmetry breaking scheme in SU(3) that brings some new isospin dependence. It also considers an effective one-gluon exchange interaction. The interaction is given by

$$V_{qq}(\vec{r})=V^{\rm OGE}(\vec{r})+V^{\rm conf}(\vec{r})+V^{\rm ch}(\vec{r}), \tag{8}$$

where $V^{\rm OGE}(\vec{r})$ and $V^{\rm conf}(\vec{r})$ are the same as in Eqs. (4) and (5), respectively. Besides, the generalization of chiral symmetry breaking generates the following Goldstone boson exchange interactions:

$$V^{\rm ch}(\vec{r})=V_{qq}^{\pi}(\vec{r})+V_{qq}^{\eta}(\vec{r})+V_{qq}^{\sigma_0}(\vec{r})+V_{qq}^{\sigma_1}(\vec{r}), \tag{9}$$

where V_{qq}^{π} and $V_{qq}^{\sigma_0}$ are the same interactions as Eqs. (6) and (7), respectively ($\alpha_{\rm ch}$ is denoted by $g_{\rm ch1}^2/4\pi$ and $\Lambda_{\rm CSB}$ by Λ_1 in the original reference). The new isospin dependence is incorporated through the potentials

$$V_{qq}^{\eta}(\vec{r})=\frac{g_{\rm ch2}^2}{4\pi}\frac{m_{\eta}^2}{4m_q^2}\frac{\Lambda_2^2}{\Lambda_2^2-m_{\eta}^2}\frac{m_{\eta}}{3}\left[Y(m_{\eta}r)-\frac{\Lambda_2^3}{m_{\eta}^3}Y(\Lambda_2r)\right]\times(\vec{\sigma}_i\cdot\vec{\sigma}_j), \tag{10}$$

$$V_{qq}^{\sigma_1}(\vec{r})=\frac{g_{\rm ch2}^2}{4\pi}\frac{\Lambda_2^2}{\Lambda_2^2-m_{\sigma_1}^2}m_{\sigma_1}\left[Y(m_{\sigma_1}r)-\frac{\Lambda_2}{m_{\sigma_1}}Y(\Lambda_2r)\right]\times(\vec{\tau}_i\cdot\vec{\tau}_j). \tag{11}$$

In all these equations,

$$Y(x)=\frac{e^{-x}}{x}. \tag{12}$$

When applied to baryons or mesons and in order to avoid an unbound spectrum, the delta function in the one-gluon exchange potential has to be regularized [21],

$$\delta(\vec{r})=\frac{1}{4\pi}\frac{e^{-r/r_0}}{r_0^2r}. \tag{13}$$

Let us remark that the radial structure of the confining potential cannot be fixed from the baryon-baryon interaction. However, the hadron spectrum is strongly dependent on the confining potential. Baryon and meson spectroscopies as well as lattice calculations [22] suggest a linear confining potential instead of quadratic, and therefore we will restrict ourselves to the use of a linear potential.

In Ref. [13] only a confining potential and a Goldstone boson exchange interaction are used, but the OGE and the scalar partners of the Goldstone bosons are not included. The interaction used is the following:

$$V_{qq}(\vec{r})=V_{\chi}^{\rm octet}+V_{\chi}^{\rm singlet}+V_{\rm conf}, \tag{14}$$

where

$$V_\chi^{\text{octet}}(\vec{r})=\left[\sum_{a=1}^{3} V_\pi(\vec{r})\lambda_i^a\lambda_j^a+\sum_{a=4}^{7} V_K(\vec{r})\lambda_i^a\lambda_j^a+V_\eta(\vec{r})\lambda_i^8\lambda_j^8\right]\times\vec{\sigma}_i\cdot\vec{\sigma}_j, \tag{15}$$

$$V_\chi^{\text{singlet}}(\vec{r})=\frac{2}{3}\vec{\sigma}_i\cdot\vec{\sigma}_j V_{\eta'}(\vec{r}) \tag{16}$$

$$V_{\text{conf}}(\vec{r})=V_0+Cr \tag{17}$$

$$V_\gamma(\vec{r})=\frac{g_8^2}{4\pi}\frac{1}{12m_im_j}\left[m_\gamma^2\frac{e^{-m_\gamma r}}{r}-4\pi\delta(\vec{r})\right],\quad \gamma=\pi,K,\eta, \tag{18}$$

$$V_{\eta'}(\vec{r})=\frac{g_0^2}{4\pi}\frac{1}{12m_im_j}\left[m_{\eta'}^2\frac{e^{-m_{\eta'}r}}{r}-4\pi\delta(\vec{r})\right]. \tag{19}$$

In this case the delta function is regularized by

$$\delta(\vec{r})=\frac{1}{4\pi}\Lambda_\gamma^2\frac{e^{-\Lambda_\gamma r}}{r}, \tag{20}$$

Λ_γ being dependent on the mass of the Goldstone boson, and therefore different for each one.

From all these potentials the $q\bar{q}$ interaction is obtained through the transformation [23]

$$V_{q\bar{q}}=\sum_\alpha (-1)^{G_\alpha}V_{qq}(\alpha), \tag{21}$$

where G_α is the G parity of the exchanged field α.

Our main concern in this context will be whether a realistic description of deeply bound states, like the pion, is compatible with a reasonable description of other observables of the one- and two-baryon systems. As we are only interested in the gross features of the meson spectra we have omitted the spin-orbit and tensor forces, which play a minor role in order to gain some simplicity.

Concerning the pion, some discussion about its nature is now in order. Chiral quark models treat the pion in two different approaches. The first one is described by Manohar and Georgi [6] when working in a nonlinear realization of the theory. The pion is identified with the elementary Goldstone boson and some *ad hoc* mechanism should be included to push the pseudoscalar $q\bar{q}$ state out of the Hilbert space. The main drawback of this scheme is that the physical pion is no longer a $q\bar{q}$ pair, its nature being very different from, for example, the ρ meson. Nevertheless, one might have hoped that the only difference between the two mesons was the internal spin structure of the quarks [6]. Another possibility would be to push the mass of the lighter $q\bar{q}$ pseudoscalar pair to the π', its first radial excitation, but one again finds the same problem.

A different point of view is that of Suzuki and Weise [24]. It consists in keeping the quarks and the Goldstone bosons structureless at the tree level, the dressing due to higher order corrections of the effective Lagrangian being responsible for the $q\bar{q}$ structure of the physical pion. Therefore, the physical pion has a $q\bar{q}$ structure while the Goldstone boson fields are structureless virtual modes [25].

These two interpretations could be distinguished through the interacting Lagrangian. The first one would be justified by a $q\bar{q}$ interaction that pushes the $q\bar{q}$ pseudoscalar configuration out of the Hilbert space. The second one implies the existence of a $q\bar{q}$ interaction that deeply binds the pseudoscalar mode to reproduce the pion mass. The parameters of the models of Refs. [8], [9], and [13] are mainly determined

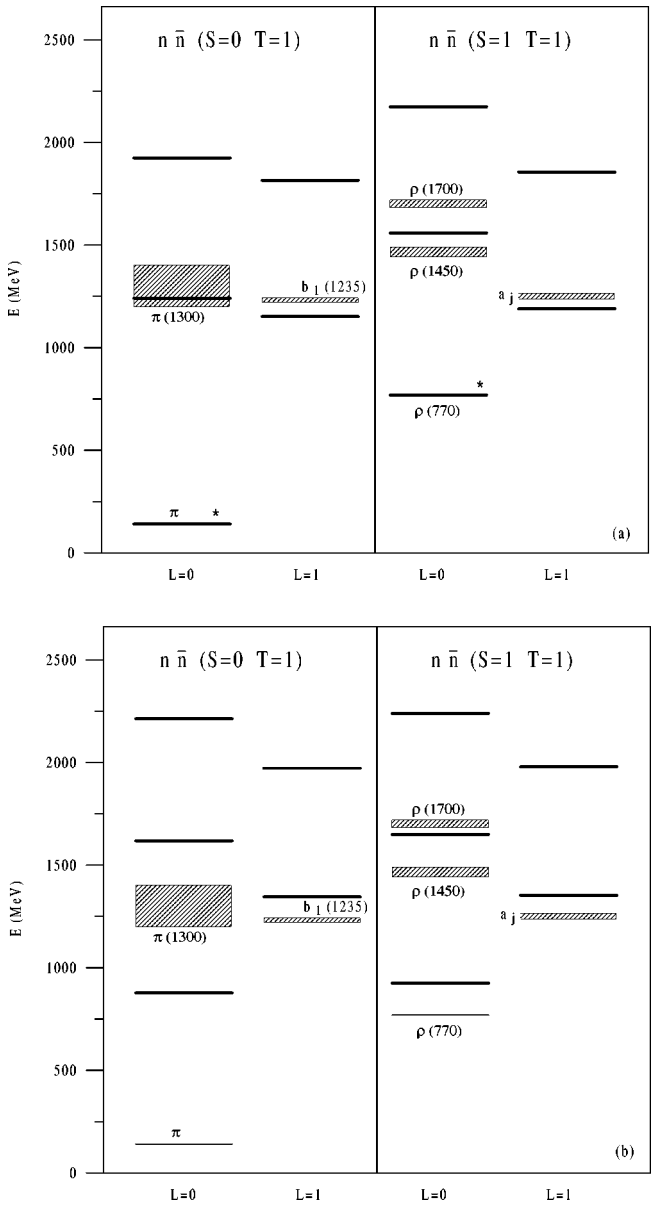

FIG. 1. (a) Comparison of experimental (shadow boxes and thin solid lines quoted with the name of the state appearing in the Particle Data Book) and calculated (solid lines) spectra of isovector mesons for the model of Ref. [8]. Experimental data are taken from Ref. [32]. *n* stands for *u* or *d* quarks. The lines labeled with a ''$\star$'' represent states where the calculated and the experimental data cannot be distinguished. The experimental data for the ^3P_J states correspond to the centroid of the multiplet. (b) Same as (a) but without including the OGE interaction.

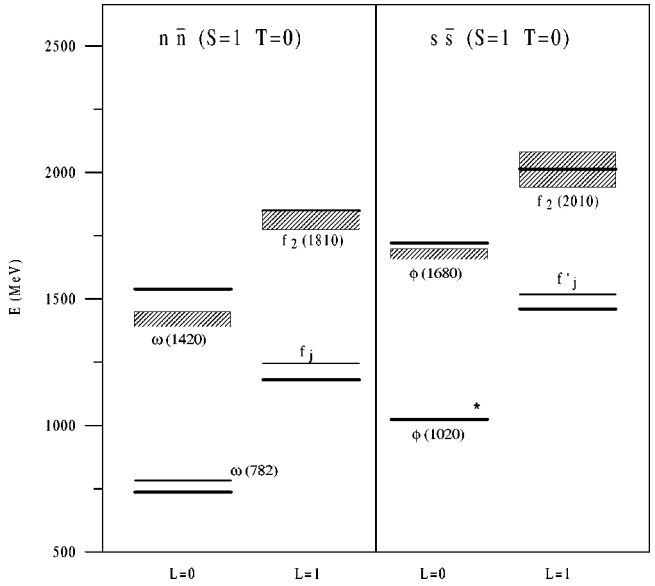

FIG. 2. Comparison of experimental (shadow boxes and thin solid lines quoted with the name of the state appearing in the Particle Data Book) and calculated (solid lines) spectra of isoscalar mesons for the model of Ref. [8]. Experimental data are taken from Ref. [32]. *n* stands for *u* or *d* quarks. The lines labeled with a ''⋆'' represent states where the calculated and the experimental data cannot be distinguished. The experimental data for the ^3P_J states correspond to the centroid of the multiplet.

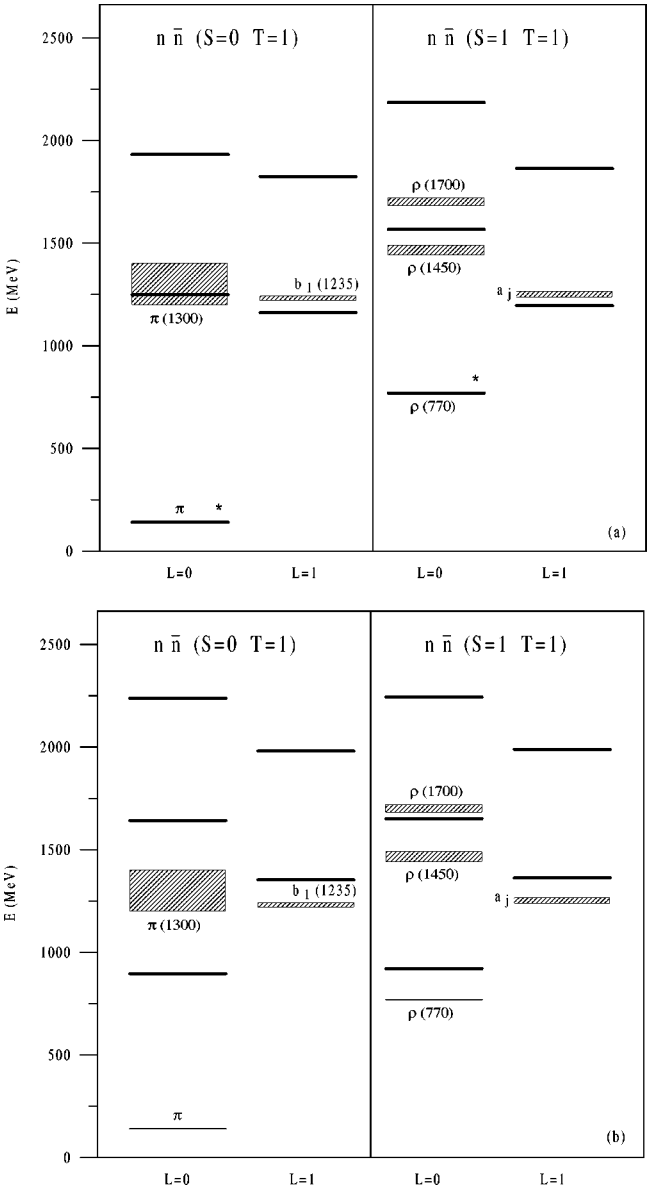

FIG. 3. (a) Same as for Fig. 1(a) but for the model of Ref. [9]. (b) Same as for Fig. 1(b) but for the model of Ref. [9].

from the one- and two-baryon problems. Therefore, through its application to the $q\bar{q}$ sector one can check if they are compatible with the existence of a deeply bound $q\bar{q}$ pseudoscalar mode that could be identified as the physical pion.

We have solved the Schrödinger equation for the three types of interactions using a standard Numerov algorithm. The quality of the results of the nonrelativistic treatment for mesons has been discussed in the literature and even compared in a very detailed way with respect to the results of semirelativistic and relativistic descriptions [26]. In particular, it has been demonstrated that there is not any advantage in a semirelativistic treatment, suggesting that this procedure must be completed by some relativization mechanism at the level of the potential [26]. Only those observables depending on the wave function at $\vec{r}=0$ need a fully relativistic treatment, like the two photon decay widths [27].

Let us first of all analyze the results of the models of Refs. [8] and [9]. In Figs. 1(a) and 2 we present the results of the model of Ref. [8] for the low-energy spectra of the isovector and isoscalar mesons, respectively. In Fig. 3(a) we show the results for the isovector mesons of the model of Ref. [9] (the results for the isoscalar mesons are similar and therefore are not shown). For the sake of consistency the results are presented using the same notation as in Ref. [18]. In both cases we have used the Yukawa-type regularization of Eq. (13) for the delta function of the OGE with a parameter $r_0=0.145$ fm and a strong coupling constant $\alpha_s=0.7$. The best fit to the experimental data is obtained with a small cutoff for the pseudoscalar interaction $\Lambda_{\mathrm{CSB}}=3.15$ fm^{-1}, although with the standard value $\Lambda_{\mathrm{CSB}}=4.2$ fm^{-1} the fit is still good. (Although we will return to these tables later on, Tables I and II illustrate the fact that the results are to a large extent independent of the value of this parameter.) As mentioned above, the confining potential is linear in both cases and the confining constant is taken to be $a_c=140$ MeV fm^{-1}. As can be seen both models provide a satisfac-

TABLE I. Mass difference, in MeV, between the π and the ρ mesons within the model of Ref. [8] when the OGE potential is switched off, as a function of the cutoff mass of the pseudoscalar exchange Λ_{CSB}. The value used in this reference is $\Lambda_{\mathrm{CSB}}=4.2$ fm^{-1}. The experimental mass difference is $m_\rho-m_\pi=630$ MeV.

Λ_{CSB} (fm^{-1})	$m_\rho-m_\pi$
2.0	28.69
3.15	47.02
4.2	60.94
5.0	70.23
6.0	80.88

TABLE II. Mass difference, in MeV, between the π and the ρ mesons within the model of Ref. [9] when the OGE potential is switched off, as a function of the cutoff masses of the Goldstone boson exchanges Λ_1 and Λ_2. The values used in this reference are $\Lambda_1=4.2$ fm^{-1} and $\Lambda_2=5.0$ fm^{-1}. The experimental mass difference is $m_\rho - m_\pi = 630$ MeV.

Λ_2 (fm^{-1}) \ Λ_1 (fm^{-1})	2.0	3.0	4.0	5.0	6.0
3.0	16.21	31.68	45.09	56.94	67.84
4.0	12.38	27.45	40.35	51.59	61.77
5.0	9.44	24.15	36.59	47.25	56.74
6.0	7.28	21.71	33.74	43.90	52.78
7.0	5.76	19.96	31.69	41.43	49.80

tory description of the meson spectra for the two sectors. They give the correct order between the states and reasonable splittings.

Although Figs. 1(a) and 3(a) look pretty similar, they are different by some MeV. The reason for the similarity between the results obtained with the models of Refs. [8] and [9] is that the only difference between the potentials is given by the additional exchange of two fields denoted by σ_1 and η in Ref. [9] and given by Eqs. (10) and (11), but they give a very small contribution to the meson spectrum. Both models provide a fit of the light meson spectra with a similar quality to that obtained with potentials specifically designed to fit the meson spectra as is the case of Refs. [15] and [18]. To illustrate this point we reproduce in Figs. 4 and 5 the results obtained in Refs. [18] and [15] for the isovector mesons, respectively. Figure 4 corresponds to Fig. 1 on p. 470 of Ref. [18], and Fig. 5 is taken from Fig. 3 on p. 194 of Ref. [15]. The validity of the model of Ref. [8] (and therefore also Ref. [9]) for higher angular momenta is checked in Fig. 6, where we show the Regge trajectories for the pion and for the rho mesons [28].

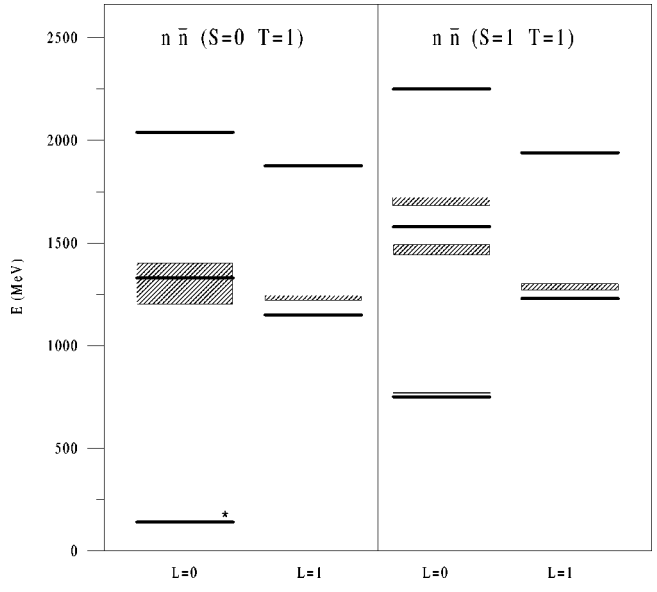

FIG. 4. Figure 1 of Ref. [18]. Comparison of the spectra of isovector mesons for the model of Ref. [18] (solid lines) and experimental data (shadow boxes and thin solid lines) taken from Ref. [32]. *n* stands for *u* or *d* quarks. The lines labeled with a ''$\star$'' represent states where the calculated and the experimental data cannot be distinguished.

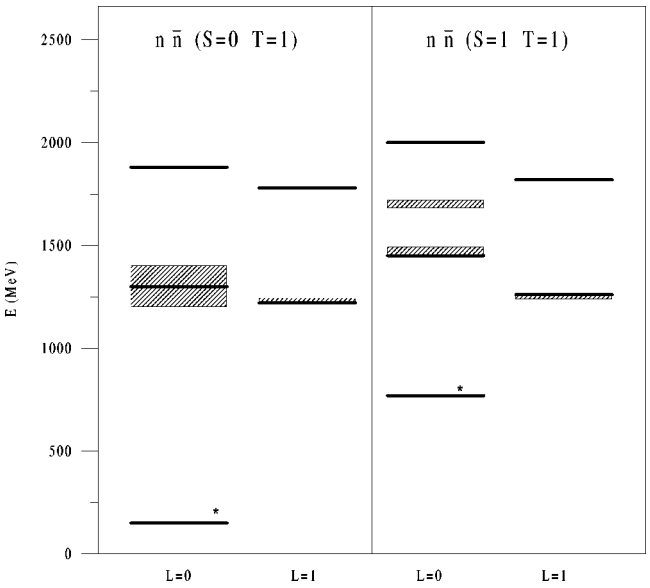

FIG. 5. Figure 3 of Ref. [15]. Comparison of the spectra of isovector mesons for the model of Ref. [15] (solid lines) and experimental data (shadow boxes and thin solid lines) taken from Ref. [32]. *n* stands for *u* or *d* quarks. The lines labeled with a ''$\star$'' represent states where the calculated and the experimental data cannot be distinguished.

Therefore, constituent quark models with chiral symmetry, which combine the short-range dynamics obtained from QCD together with the long-range aspects generated by chiral symmetry breaking, have enough structure to allow for an understanding of the general features of the light meson spectra. Some general problems are still present in these

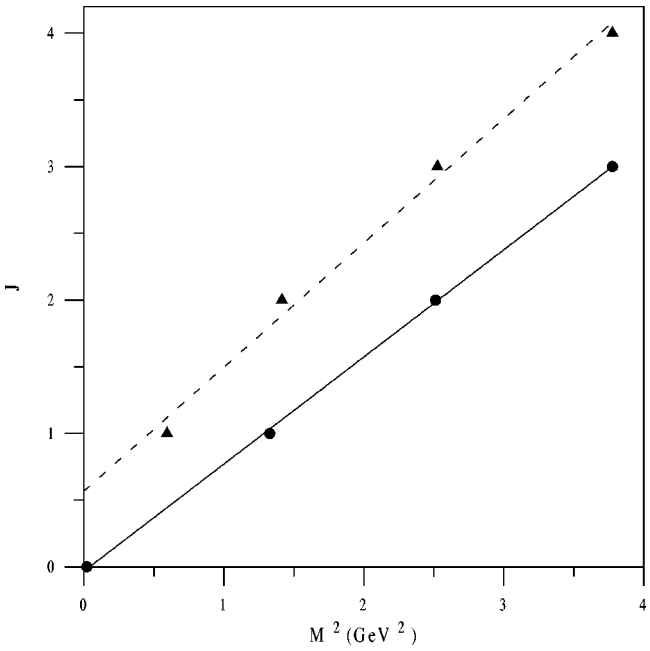

FIG. 6. Regge trajectories for the pion (solid line) and for the rho meson (dashed line) obtained with the model of Ref. [8]. Experimental data (circles and triangles) are taken from Ref. [32].

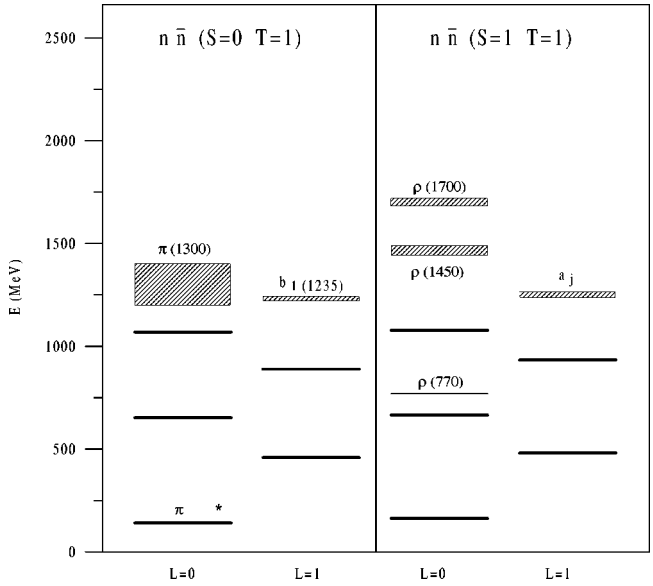

FIG. 7. Same as for Fig. 1(a) but for the model of Ref. [13].

simple approaches, as, for example, the fact that they do not describe correctly the splitting between the π and η and η' mesons, although it is known that these masses are reproduced if one considers, for example, an instanton-based model obtained from the 't Hooft interaction even in a nonrelativistic reduction [27,29]. This type of interaction includes a color-spin-dependent term similar to the OGE [30].

The important feature we want to emphasize is what happens if the color-spin-dependent interaction of the chiral quark cluster models is not present. Then, we are led to an unwanted situation that also takes place in models without color-spin-dependent forces as, for example, that of Refs. [10] and [13]. An interesting experimental finding for the light mesons is the constancy of the difference of the squared masses of the corresponding spin-singlet and spin-triplet states $\Delta M^2 \equiv M^2(^3S_1) - M^2(^1S_0)$. As shown in Figs. 1(a) and 3(a), in the models of Refs. [8] and [9] this mass difference is reproduced. However, the model of Refs. [10] and [13] leads to degenerate $^3S_1$ and $^1S_0$ states, as can be seen in Fig. 7 where we show the results of the model of Ref. [13] for the isovector mesons.

The same effect is observed in the models of Refs. [8] and [9] when the OGE interaction is switched off. We display in Figs. 1(b) and 3(b) the results for these two models when the OGE is not considered. In this case, the mass difference between the ground state of $S=0$ and $S=1$ is much smaller than the experimental one; in fact they have almost the same energy. Besides, this degeneracy, induced by the absence of color-spin-dependent forces, cannot be changed magnifying the spin-dependent interactions of the models, the only ones which could solve this discrepancy. When the OGE is not considered in the model of Refs. [8] and [9], we give in Tables I and II the dependence of the mass difference between the π and ρ mesons on the cutoff of the spin- and spin-isospin-dependent interactions, when they are taken as free parameters, trying to force the model to describe the experimental mass difference. The same result is shown in Table III for the model of Ref. [13] (which never considers the presence of the OGE) when the cutoff of the η' is taken to be free. As can be seen, none of these type of forces is able to produce the correct splitting between the $^1S_0$ and the $^3S_1$ states with a reasonable set of parameters.

TABLE III. Mass difference, in MeV, between the π and the ρ mesons within the model of Ref. [13] as a function of the cutoff mass of the η'. The value used in this reference is $\Lambda_{\eta'} = 6.8$ fm^{-1}. The experimental mass difference is $m_\rho - m_\pi = 630$ MeV.

$\Lambda_{\eta'}$ (fm^{-1})	$m_\rho - m_\pi$
4.0	30.17
5.0	26.26
6.0	23.63
7.0	21.87
8.0	20.71

Responsible for the success of the models of Refs. [8] and [9] is the color-spin structure of the residual interaction, usually attributed to the OGE, which is not present in the model of Refs. [10] and [13]. This dependence is able to explain the splitting between the pseudoscalar (π) and vector mesons (ρ), and also that between the octet (N) and decuplet (Δ) baryons [31]. One should take into account that any other interaction with this color-spin structure would generate a similar effect. For example, the instanton-induced interaction deduced in Ref. [30], although with a different origin than the OGE, has its same characteristic color-spin structure and therefore similar results are obtained [18].

To conclude, if the OGE is not considered, chiral quark models predict that the ground states of the $S=0$ and $S=1$ isovector mesons are degenerated [see Figs. 1(b), 3(b), and 7], something for which there is no experimental evidence. When the color-spin structure of the OGE is taken into account, the $S=0$ pseudoscalar mode is deeply bound [see Figs. 1(a) and 3(a)], allowing us to understand the presence of a $q\bar{q}$ pair with such a low mass as that of the pion. As a consequence, the most important point extracted from this study has to do with the structure of the quark-quark interaction. In principle there is no reason to rule out or to justify the inclusion of the exchange of gluons, instantons, or any degree of freedom related to the realization of QCD at low energy. These terms of the interaction are found to be fundamental in the literature for other purposes, the first one to explain the short-range behavior of the NN interaction and the second to solve the $U_A(1)$ anomaly. We have found that the main aspects of the meson spectra can be understood if the chiral quark models include the OGE due to its characteristic color-spin structure. The presence of a QCD-inspired force like the OGE or the instanton-induced interaction seems to be important to explain in this framework the existence of deeply bound states like the pion together with other observables of one- and two-hadron systems.

ACKNOWLEDGMENTS

This work has been partially funded by Dirección General de Investigación Científica y Técnica (Spain) under Contract No. PB94-0080. L.A.B. acknowledges the Ministerio de Educación y Cultura (Spain) for financial support.

[1] W. Lucha, F. Schröberl, and D. Gromes, Phys. Rep. **200**, 127 (1991), and references therein.
[2] K. Shimizu, Rep. Prog. Phys. **52**, 1 (1989), and references therein.
[3] A. de Rújula, H. Georgi, and S.L. Glashow, Phys. Rev. D **12**, 147 (1975).
[4] G. 't Hooft, Phys. Rev. D **14**, 3432 (1976); M.A. Shifman, A.I. Vainshtein, and V.I. Zakharov, Nucl. Phys. **B163**, 46 (1980); E.V. Shuryak, Phys. Rep. **115**, 151 (1984).
[5] H. Suganuma, S. Sasaki, and H. Toki, Nucl. Phys. **B435**, 207 (1995).
[6] A. Manohar and V. Georgi, Nucl. Phys. **B234**, 189 (1984).
[7] M.D. Scadron, Yad. Fiz. 56, 245 (1993) [Phys. At. Nucl. **56**, 1595 (1993)].
[8] F. Fernández, A. Valcarce, U. Straub, and A. Faessler, J. Phys. G **19**, 2013 (1993).
[9] Y.W. Yu, Z.Y. Zhang, P.N. Shen, and L.R. Dai, Phys. Rev. C **52**, 3393 (1995).
[10] Fl. Stancu, S. Pepin, and L. Ya. Glozman, Phys. Rev. C **56**, 2779 (1997).
[11] I.I. Obukhovsky and A.M. Kusainov, Phys. Lett. B **238**, 142 (1990).
[12] A. Valcarce, P. González, F. Fernández, and V. Vento, Phys. Lett. B **367**, 35 (1996).
[13] L. Ya. Glozman, Z. Papp, W. Plessas, K. Varga, and R.F. Wagenbrunn, Phys. Rev. C **57**, 3406 (1998).
[14] V.G. Neudatchin, Yu.F. Smirnov, and R. Tamagaki, Prog. Theor. Phys. **58**, 1072 (1977).
[15] S. Godfrey and N. Isgur, Phys. Rev. D **32**, 189 (1985).
[16] E.V. Shuryak, Nucl. Phys. **B214**, 237 (1983).
[17] W.H. Blask, U. Bohn, M.G. Huber, B.Ch. Metsch, and H.R. Petry, Z. Phys. A **337**, 335 (1990).
[18] C. Semay and B. Silvestre-Brac, Nucl. Phys. **A618**, 455 (1997).
[19] E. Shuryak and T. Schäfer, Annu. Rev. Nucl. Part. Sci. **47**, 359 (1997).
[20] D.I. Dyakonov and V.Yu. Petrov, Nucl. Phys. **B272**, 457 (1986).
[21] R.K. Bhaduri, L.E. Cohler, and Y. Nogami, Phys. Rev. Lett. **44**, 1369 (1980).
[22] F. Gutbrod and I. Montway, Phys. Lett. **136B**, 411 (1984).
[23] J.S. Ball and G.F. Chew, Phys. Rev. **109**, 1385 (1958); J. Burger, R. Müller, K. Tragl, and H.M. Hofmann, Nucl. Phys. **A493**, 427 (1989).
[24] K. Suzuki and W. Weise, Nucl. Phys. **A634**, 141 (1998).
[25] A.W. Thomas, Adv. Nucl. Phys. **13**, 1 (1984).
[26] C. Semay and B. Silvestre-Brac, Phys. Rev. D **46**, 5177 (1992).
[27] C.R. Münz, J. Resag, B.C. Metsch, and H.R. Petry, Nucl. Phys. **A578**, 418 (1994).
[28] L.A. Blanco, Diploma thesis, University of Salamanca (unpublished).
[29] E. Klempt, B.C. Metsch, C.R. Münz, and H.R. Petry, Phys. Lett. B **361**, 160 (1995).
[30] M. Oka and S. Takeuchi, Nucl. Phys. **A524**, 649 (1991).
[31] P.J. Mulders, Phys. Rep. **185**, 83 (1990).
[32] Particle Data Group, R.M. Barnett *et al.*, Phys. Rev. D **54**, 1 (1996).